

SECM imaging of electrocatalytic activity for oxygen reduction reaction on thin film materials

Guojin Lu^{*}, James S. Cooper, Paul J. McGinn

*Department of Chemical and Biomolecular Engineering and Center for Molecularly Engineered Materials,
University of Notre Dame, Notre Dame, IN 46556, United States*

Received 11 December 2006; received in revised form 6 February 2007; accepted 8 February 2007
Available online 16 February 2007

Abstract

The oxygen reduction reaction (ORR) on sputtered Pt thin films in acidic solution was successfully studied by scanning electrochemical microscopy (SECM) in a modified tip generation–substrate collection (TG–SC) mode. SECM images of ORR activity in different sample areas were obtained and it is shown that this TG–SC SECM technique can be used to screen electrocatalytic activity of continuous thin film samples efficiently and quickly for the ORR in an acidic medium. It is observed that this technique is not very sensitive to the tip–substrate separation within a certain range. The SECM images obtained are strongly dependent on the substrate potential. The advantages of this technique for studying ORR electrocatalysts are discussed.

© 2007 Elsevier Ltd. All rights reserved.

Keywords: PEM fuel cells; Scanning electrochemical microscopy (SECM); Tip generation–substrate collection (TG–SC) mode; Oxygen reduction reaction (ORR); Combinatorial discovery

1. Introduction

Although steady progress has been achieved in the development of polymer electrolyte membrane (PEM) fuel cells, their commercialization is still challenged by several factors. Performance of PEM fuel cells is mainly limited by the insufficient activity of the fuel cell electrodes. The design of a high-performance and less-costly cathode material for the ORR is critical to that issue because the kinetics of the ORR are much slower than that of the hydrogen oxidation reaction (HOR) or the methanol oxidation reaction (MOR) [1,2].

Combinatorial materials synthesis and high-throughput screening have been applied to systematically and rapidly identify candidate electrocatalyst materials for PEM fuel cells [3–10]. In previous publications, we described a plasma sputtering system for the deposition of combinatorial catalyst libraries for PEM fuel cells, and the quantitative screening of their electrocatalytic activity (reactivity imaging) by SECM [11–14]. These research efforts have shown that SECM is a versatile analytical

technique to perform imaging of electrocatalytic activity variation as a function of composition in a planar combinatorial library.

Pt-based alloys, especially Pt–TM (transition metals, such as Ni, Co, Cr, Fe, etc.) alloys are currently considered as optimum ORR catalytic materials. Despite the lack of agreement on the factors leading to improvements in Pt–TM alloys, a key feature of these alloys is that they typically couple Pt with a metal whose surface oxide formation onset potential is more positive than Pt. This forms the basis for most strategies for developing improved catalysts. A strategy for selecting possible catalysts has recently been suggested by Fernandez et al. [15]. They recommend combining a metal that can easily break the O–O bond of O₂ (forming adsorbed atomic oxygen) with a metal that will easily reduce the adsorbed atomic oxygen and showed the suitability of the guidelines by examining additions of Co to Pd, Au, and Ag. These materials selection guidelines have more recently been extended by thermodynamic calculations by Wang and Balbuena [16].

Despite the advantages of using combinatorial screening methods to discover novel electrocatalytic materials for PEM fuel cells, only a few combinatorial investigations and even fewer studies using SECM as the screening tool for the ORR can be found in the literature [15,17–20]. The difficulty in using

^{*} Corresponding author.
E-mail address: glu1@nd.edu (G. Lu).

SECM is that the ORR in an acidic solution cannot be studied efficiently in feedback mode, which is typical for most SECM practice. The ORR in acidic solution can be expressed as in Eq. (1). Since water (H_2O), which is plentiful in the bulk solution and around the tip, is the oxygen reduction reaction product, its feedback diffusion to the tip will not cause tip current to change.



Imaging of electrocatalytic activity for oxygen reduction in an acidic medium by SECM was first successfully achieved by Bard and co-workers on discrete catalyst spots on glassy carbon prepared by reduction of precursors with sodium borohydride [15,19], where a modified tip generation–substrate collection (TG–SC) SECM mode was proposed as an alternative operation mode for feedback mode. The principle is shown in Fig. 1, and is compared with that of a typical feedback mode for the hydrogen oxidation reaction. In the HOR feedback mode, the substrate potential is set at a certain potential at which molecular hydrogen can be oxidized, while the tip is typically held at another constant potential at which the tip reaction is the diffusion-limited reduction of protons to generate hydrogen. At a very small tip–substrate separation, the tip-generated hydrogen can diffuse to the surface of the substrate sample, where it can be oxidized, creating a proton on an electrochemically active surface. Generated protons can then diffuse back to the tip surface where they are reduced, resulting in additional tip current. Accordingly, the difference in relative tip current with position reflects the activity difference of the local sites of the substrate toward hydrogen oxidation. In this mode, it is the tip current that is detected and monitored.

In the modified ORR TG–SC mode, a constant oxidation current is applied from an external circuit to the tip so that oxygen can be generated at the tip (i.e. tip generation (TG)) and diffuse to the substrate, which is fixed at a potential where oxygen can be reduced on ORR active areas on the substrate (i.e. substrate collection (SC)). Since the tip current is not controlled by the bi-potentiostat/galvanostat itself, but by an external circuit, this technique is called a modified TG–SC mode SECM. In this mode, it is the substrate current instead of the tip current that is monitored. By measuring and comparing the current signals

from local areas on the substrate, ORR catalytic activity from different areas on the substrate can be mapped.

In the present study, modified TG–SC mode SECM is applied to investigate ORR activity on continuous thin film catalyst layers of Pt prepared by sputter deposition on a Si wafer, instead of discrete spots as in the work by Fernandez and Bard [19]. This represents a first step before applying the technique to more complex composition spread films as utilized in combinatorial materials studies.

2. Experimental

2.1. Catalyst sample preparation

Thin metal stripes were prepared by plasma sputtering onto a 2 in. silicon wafer. Prior to deposition, a 1000 Å Si oxide film was thermally grown on the surface. A base layer of 2000 Å-thick TiN was deposited by reactive sputtering onto the wafer to act as a diffusion barrier and electrode contact. Pt (99.99% target purity) was then sputtered through a simple offset masking approach [13,14]. The width of the hole on the mask is 0.6 mm. Stripes of ~6 mm length, ~1 mm width, and ~160 Å thick were deposited. Since the mask is not in contact with the substrate (offset), the film thickness tapers away at the edges. Thus the width and length of the stripes cannot be accurately determined, as it depends on defining a cut-off thickness.

2.2. Scanning electrochemical microscopy characterization

Pt stripes were characterized for their electrochemical activity towards the ORR with a system consisting of a scanning electrochemical microscope (UniScan SECM 270) and PG580R potentiostats controlled by a computer. A homemade Au microelectrode with a 25 µm diameter was used as the probe. The microelectrode tip employed in the SECM was fabricated with a 25 µm diameter Au wire (Alfa Aesar) sealed in glass. The Au wire was first inserted into a borosilicate capillary tube (3 mm o.d., 50 µm i.d., 5 mm long, provided by VitroCom) and was then heated. After the capillary collapsed onto the wire, the tip was continuously heated until the capillary fused to a long 3 mm

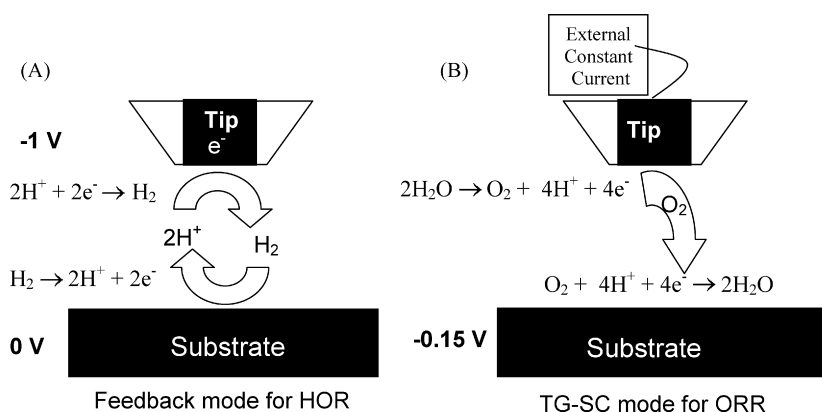


Fig. 1. Schematic diagrams of the SECM working under feedback mode for studying HOR (A) and under the current modified TG–SC mode for studying ORR in acidic medium (B).

o.d. (i.d. 1.6 mm) regular glass tube with the help of a vacuum pump. The tip was then polished to form a cone at an angle greater than 45° on a modified Ultra-tec polishing machine, and finally polished manually with $6\text{ }\mu\text{m}$, $1\text{ }\mu\text{m}$, $0.1\text{ }\mu\text{m}$ diamond and $0.05\text{ }\mu\text{m}$ alumina. The final structure has a glass to metal ratio greater than 10:1. Electrical contact between the gold wire and a Cu contact wire was made through indium powder by heat melting. Following polishing, the tip was cleaned with acetone, alcohol, and distilled water and stored submerged in the solution of $0.01\text{ M H}_2\text{SO}_4/0.1\text{ M Na}_2\text{SO}_4$ before use.

Fig. 2 shows the scheme of the electrochemical experimental setup. The electrochemical cell was composed of four electrodes with the tip as the oxygen generator and the sample substrate (Si wafer) as the working electrode. A saturated calomel electrode (SCE, 0.242 V versus SHE) and Pt mesh were used as the reference electrode and counter electrode, respectively. In the description that follows, all the potentials refer to SCE if not otherwise stated. The constant external positive current of the tip was controlled with two 9 V batteries in series (the actual voltage is about 10.6 V) and a $50\text{ M}\Omega$ resistor between the tip and the counter electrode. The nA scale tip current was monitored by a Keithley 614 electrometer. The substrate was positioned at the bottom of the cell horizontally with the deposited surface facing upwards. Sealing of the home-made electrochemical cell was made secure by rubber O-rings fitted into grooves at both the top and the bottom of the cell. During the electrochemical experiments, only a limited area of TiN and Pt stripe was exposed to the solution. Pattern transfer was achieved by photolithography in a clean room environment. The metallized Si wafer was coated with a layer of Shipley 1813 photoresist through a spin-coating procedure. The photoresist layer was then exposed to radiation from a mercury vapor lamp after alignment in a Karl Suss mask aligner. Resist development results in opening a 3 mm diameter circle as illustrated in Fig. 3, so that only a part of a Pt stripe is exposed to the electrolyte during the electrochemical experiments, with most of the metallized wafer remaining covered by the photoresist. The contact lead for the substrate electrode was connected through the edge of the TiN covered Si wafer, which

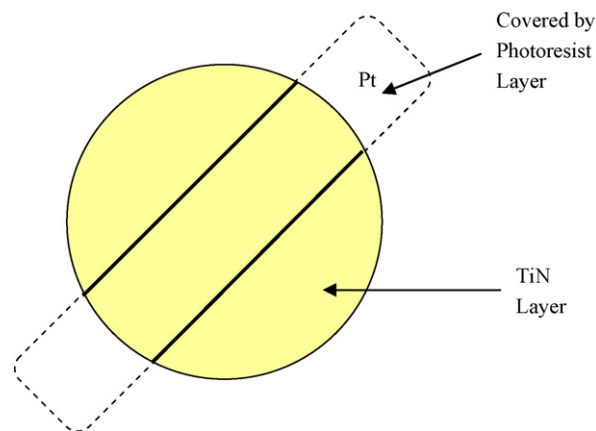


Fig. 3. Sample profile for a Pt stripe (length 6 mm , width $\sim 1\text{ mm}$) on a photoresist-covered 2 in. Si wafer. Areas outside the circle on the Si wafer including areas in the dashed lines are covered by photoresist. The diameter of the circle that is not covered by photoresist is 3 mm .

is free of photoresist and located outside of the cell and therefore not in contact with the solution.

After the substrate was placed in the cell, it was leveled so that the sample surface was parallel to the x - y plane traversed by the microelectrode tip. The solution of $0.01\text{ M H}_2\text{SO}_4/0.1\text{ M Na}_2\text{SO}_4$ electrolyte was first introduced into the cell. Before conducting ORR catalytic characterization experiments, the tip was cleaned by sweeping cyclic voltammetry (CV) between -1.2 V and $+1\text{ V}$ at a scan rate of 50 mV s^{-1} for 10 cycles with the tip located at a long distance (over $500\text{ }\mu\text{m}$) from the substrate. After cleaning, the steady-state tip current ($I_{T,\infty}$) was approximately -400 nA at -1 V . Following the tip cleaning procedure, an approach curve was measured to determine the tip–substrate separation. Then an HOR feedback image of the stripe(s) was obtained to precisely locate the tip at the area of interest with the tip set $10\text{ }\mu\text{m}$ above the substrate surface [14]. Following this, the electrochemical cell was rinsed with milli-Q water and $0.5\text{ M H}_2\text{SO}_4$ solution was introduced into the cell and the tip was positioned above the substrate with the desired tip–substrate separation. ORR characterization of the samples was then performed in the modified TG–SC mode. For the Pt stripe, a surface area of $3\text{ mm} \times 3\text{ mm}$ in the x and y directions was scanned at a scan step size of $50\text{ }\mu\text{m}$ and a scanning rate of $50\text{ }\mu\text{m/s}$. The tip oxidation current (I_{tip}) was kept around 180 nA , and the substrate was held at a potential (E_{sub}) in the range between 0.2 and -0.25 V , where oxygen can be reduced. The substrate current was directly monitored as the tip was scanned across the substrate. The current is larger when the oxygen-generating tip is located over more ORR active areas, so the relative change with position permitted ORR imaging of the substrate.

Before each scanning experiment, the substrate was cleaned by CV sweeping between 0.5 and -0.3 V at a scan rate of 50 mV s^{-1} for 10 cycles. To avoid interference from dissolved oxygen from the air, the electrolyte was deaerated by bubbling N_2 for 30 min with the upper opening of the cell covered by parafilm (Fisher Scientific), leaving only a small hole for the tip to penetrate. During the experiments, a N_2 blanket was established by continuous flow above the solution.

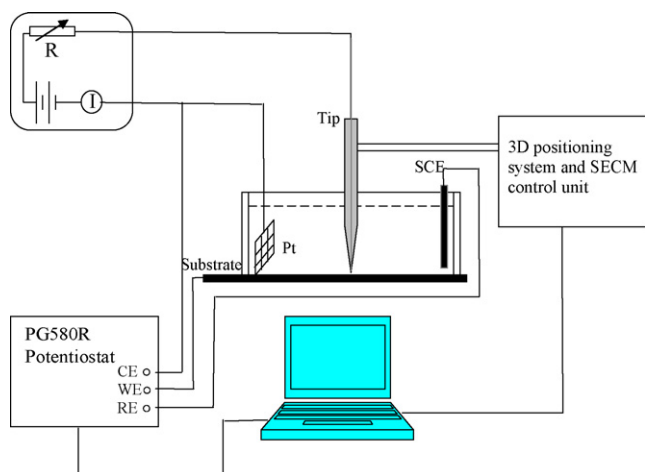


Fig. 2. Schematic diagram of the electrochemical setup used for the modified TG–SC mode SECM experiments.

2.3. AFM measurements

The surface topography of selected areas of the Pt stripe was characterized using a Digital Instruments Multimode III atomic force microscope. The AFM measurements were carried out in air with the AFM operating in the tapping mode.

3. Results

3.1. Design of the electrochemical system

Our initial efforts to study oxygen reduction by the TG–SC mode were not successful. There was substantial electronic noise so that the signal from the ORR on the substrate could not be differentiated, especially when the substrate current (signal plus noise) was less than 1 μA . Two main problems were identified and corrected. The electrochemical setup initially employed was the one designed for use in feedback mode SECM, which uses a “fish-hook” platinum wire that is immersed in the electrolyte to make electrical contact to the substrate, similar to the cell design described in [21]. That system resulted in large electronic noise relative to the substrate current, which is of the μA or even nA scale. In feedback mode, it is the tip current instead of the substrate current that is monitored, so high substrate current noise is not a concern. However, in TG–SC mode, the substrate current is of prime interest and its accuracy is very important to evaluate the ORR reaction rate at different locations on the substrate.

This problem was remedied by redesigning the electrochemical cell. Instead of a Pt wire contacting the TiN in the electrolyte, the contact to the substrate TiN layer was made outside of the cell or the electrolyte. Redesign of the nA–current source resulted in further noise reduction. Initially we used a nanocurrent source built according to [21], but it was found that connecting that electronic circuit between the tip and the counter electrode triggered high noise current, the reason for which remains unclear. Instead a much simpler circuit employing a battery and a M Ω resistor solved the problem, resulting in a tolerable noise level and a relatively stable current signal.

Further signal optimization was achieved by masking off most of the conductive area on the substrate surface. The stripes are on a conductive, TiN-coated 2 in. diameter Si wafer, so the background current is large compared to the current from the reduction of oxygen diffused from the tip. In our early efforts, the background current was 1–10 μA when the substrate potential was from 0.2 to -0.2 V. That background current range is obviously too large for the oxygen generation current from the tip, which should be less than 220 nA to avoid oxygen bubble formation due to oxygen saturation [19]. In order to be compatible with the SECM and have enough room for the electrochemical setup, the size of the substrate cannot be minimized too much, but the conducting area (TiN layer) of the substrate has to be decreased. The main source of the background current is probably from the reduction of impurities and oxides on the substrate, as well as oxygen (from air) remaining in the solution. Thus, the TiN exposure was minimized through the use of photoresist masking as described above. Through this experimental refine-

ment the background current is dramatically decreased to less than 200 nA for the applied substrate potential range.

3.2. SECM images for ORR

With the new cell and sample design, SECM images can be obtained for the ORR during a TG–SC mode experiment on a Pt stripe, as shown in Fig. 4A, where the substrate current is represented by color and plotted as a function of tip position (x and y coordinates). The tip–substrate separation (d) in this case was 15 μm and the substrate potential was kept at -0.15 V. When the tip passes over the ORR active Pt surface, the substrate current notably increases. This SECM image shows the shape and the size of the Pt stripe with fairly good resolution.

The circular shape of the exposed TiN layer can be detected in Fig. 4A and is approximately outlined by the dashed white circular line. Detection of the TiN layer means that it also has some ORR activity, although much lower than that of Pt. This may indicate that the TiN layer is slightly non-stoichiometric (TiN_{1-x}) resulting in some titanium oxide in this layer. This oxide is known to exhibit some electrocatalytic activity towards the ORR when the potential is more negative than a specific onset potential, which is about 0.14 V in the current system [22]. For example, the SECM image in Fig. 4B does not show the circular shape of the exposed TiN layer when the substrate potential is kept at 0.2 V, at which titanium oxide exhibits no ORR activity. However, the signal from the Pt stripe is now greatly diminished.

It is noted that the background current tends to increase gradually with the scanning time across a sample (in the figures shown here, scanning occurs from bottom to top). The background current in Fig. 4A is initially about 80 nA and increases gradually with the tip scanning to about 100 nA at the end of the area scan. The image in Fig. 4A can be seen to become noisier toward the top. A possible reason is that there is an accumulation of unreacted oxygen since oxygen generated from the tip cannot always be totally reduced on the substrate. All of the oxygen from the tip cannot reach the substrate surface, since there will be some oxygen diffusing into the bulk solution. The oxygen that reaches the substrate can only be reduced on an ORR-active spot, and not all of this oxygen will be reduced. The gradual background current increase also may be the result of oxygen leaking from outside of the cell with time. Although the cell is sealed by parafilm and the solution in the cell is protected by a N_2 blanket, a micro-leak of O_2 from outside of the cell is still possible.

This time-dependent effect is detrimental to the relative contrast in the SECM image and should be eliminated to the largest extent. One possible approach is to decrease the time for each experiment, either by increasing the scan rate or by further decreasing the sample size, hopefully without sacrificing the accuracy of the characterization. For this reason, current efficiency is calculated with the data from the early part of a scan. For example, the maximum current efficiency can be estimated as 87.6% (155/177) by dividing the tip oxidation current (178 ± 3 nA) by the maximum net substrate current (maximum current minus the background current), from a line scan as shown in Fig. 4C, which is along the line of y coordinate -0.6 mm.

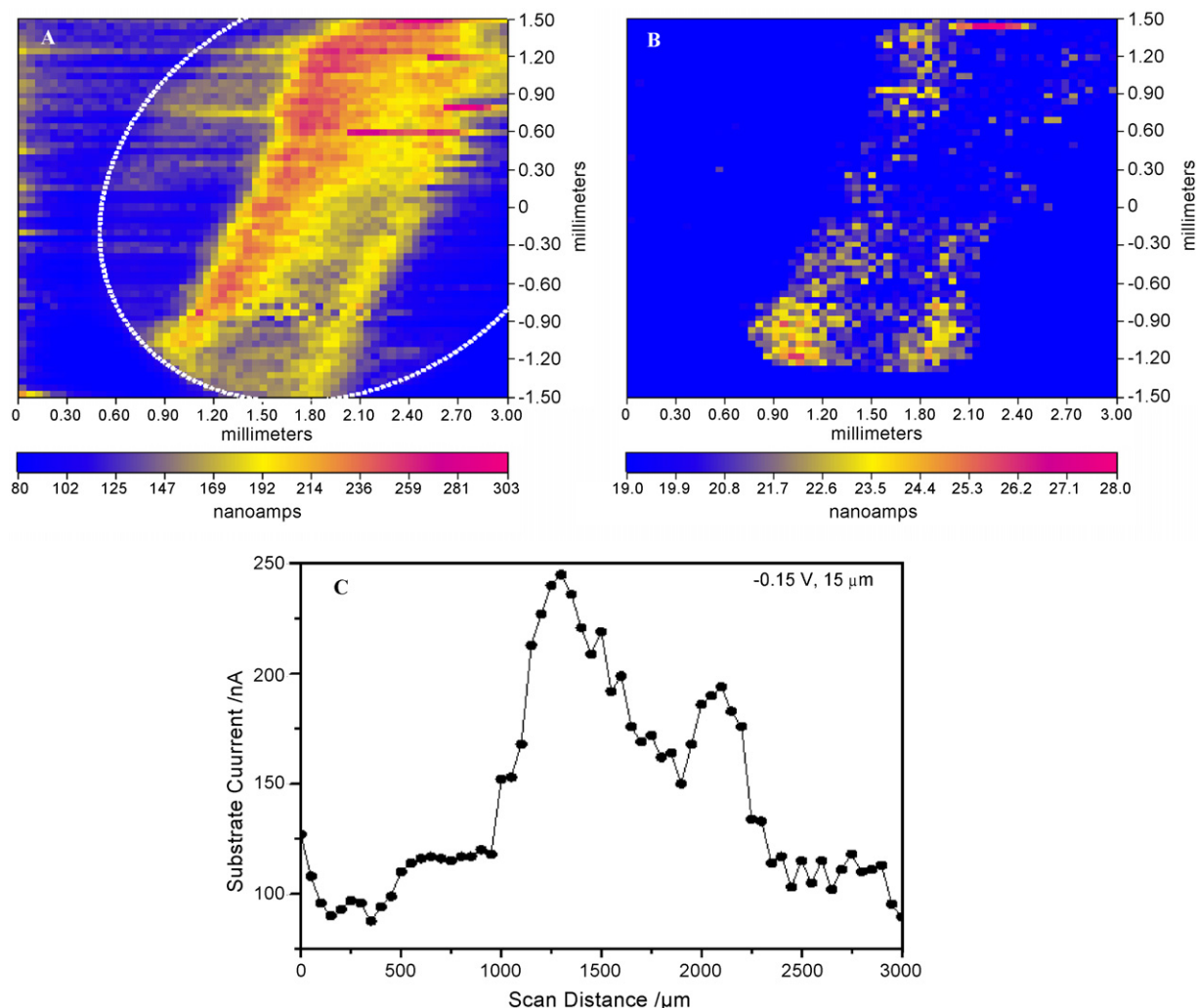


Fig. 4. (A) A typical area scan ORR image obtained by TG–SC SECM of a Pt stripe in 0.5 M H_2SO_4 : $E_{\text{sub}} = -0.15 \text{ V}_{\text{SCE}}$, $I_{\text{tip}} = 177 \text{ nA}$, $d = 15 \mu\text{m}$. (B) Image obtained with substrate potential at $0.2 \text{ V}_{\text{SCE}}$, $I_{\text{tip}} = 181 \text{ nA}$, $d = 15 \mu\text{m}$. (C) A line scan from (A) along the line of y coordinate of -0.6 mm .

It is also noted in Fig. 4A and many SECM ORR images shown later that the ORR activity at the edge of the Pt stripe is larger than that in the center in most cases. Similar observations can also be made for SECM images of the HOR [14]. The reason for this “edge effect” is thought to be the result of varying film thickness through the cross section of the stripe. The Pt thickness parallel to the stripe axis is uniform, but the thickness varies perpendicular to the stripe axis [14]. The gradient in thickness can produce a varying microstructure, resulting in non-uniform ORR activity. To investigate this “edge effect”, AFM images of both edge and center areas on the Pt stripe were obtained and are presented in Fig. 5. It is seen that there is a difference in the structure of the film in the two areas. The columnar structure in the center of the stripe where the film is thicker appears more densely packed, compared to the edge where the film tapers away. The center is generally smoother, as shown by the range of column height in the scale to the right of the figure. Surface roughness of these two AFM images was analyzed by calculating the ratio of the real area (three-dimensional) to the geometric (projected) area of the surfaces using a proprietary Nanoscope III 5.12r3 software, which is associated with the AFM instru-

ment. The three dimensional area was determined by joining the experimentally acquired height data in a triangular net and approximating the real area with the sum of the areas of the triangles thus formed. Root mean square roughness of 3.63 for the edge and 1.68 for the center were obtained. As the result of the varying film thickness, the surface area at the stripe edge where the film is thinner is larger than that in the center. This difference in surface area (from the center to the edge of the Pt stripe) results in the increased near-edge activity seen in the stripes.

3.3. The effect of substrate potential on SECM images

When the ORR is investigated with the SECM system, the image resolution and quality should theoretically depend on the substrate potential. While the oxygen reduction current (and therefore the ORR current efficiency) increases with decreasing substrate potential (more negative), the background current should also gradually increase with decreasing substrate potential. If the substrate potential is higher than a certain level, the ORR activity at some locations can be close to zero, although Pt may be present there. Meanwhile, with a decreasing substrate

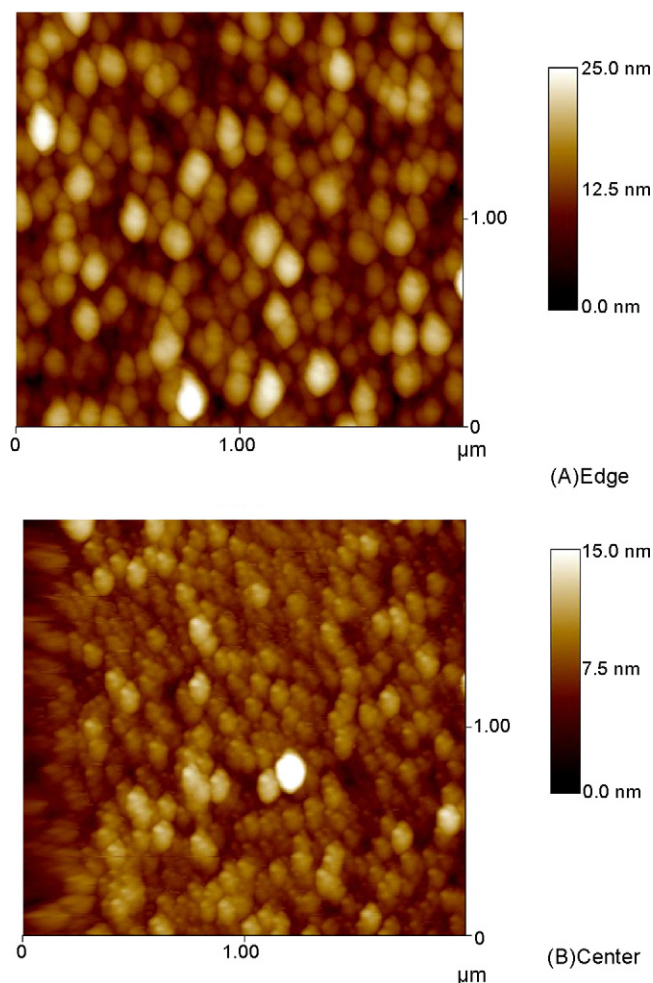


Fig. 5. AFM topographic images ($2\ \mu\text{m} \times 2\ \mu\text{m}$) of different areas on the Pt stripe: (A) near the edge and (B) in the center.

potential, the kinetics of the ORR on Pt will transition from electrochemical activation controlled to mixed control (with diffusion control) and then finally to being totally diffusion controlled. Below a certain potential, further decreasing the substrate potential will not result in additional ORR current from the substrate.

Based on the above considerations, an initial increase followed by a decrease of the ORR current efficiency is expected. To examine this expectation, the effect of substrate potential on the SECM image was investigated and the results are shown in Fig. 6, where SECM images with substrate potentials of 0.1, 0, -0.15 and -0.25 V are presented. Corresponding line scan results along the line of y coordinate -0.6 mm from those images were analyzed (not shown), from which the maximum ORR current efficiency can be calculated. The maximum net substrate current for each case was plotted as a function of substrate potential and is presented in Fig. 7. As expected, the current efficiency increases with decreasing substrate potential, as the ORR electrokinetics increase with increasing overpotential. However, the maximum net substrate current is almost constant when the substrate potential is more negative than -0.15 V, which indicates that the ORR transitions from activation controlled to diffusion

controlled. Again, it is observed that the background current increases gradually during the scan and is dependent on the substrate potential. In all cases, the calculated current efficiency is less than 100% at even the most negative substrate potential, since the faradic efficiency for both oxygen evolution on the tip and oxygen reduction on the substrate is smaller than 100% because of secondary reactions, such as the generation of hydrogen peroxide or other intermediate species [19]. Reduced efficiencies may also be due to the oxidation of impurities in the electrolyte on the tip, or some extent of deactivation of the Pt surface because of contamination from the electrolyte.

Although reasonably clear SECM images can be obtained at all different substrate potentials, as shown in Fig. 6, it is observed that the image contrast ratio between current from the ORR on the surface of substrate and the background current for more negative potentials is larger than at more positive potentials, which is important, especially when the currents for the Pt stripe and the TiN layer have to be differentiated. The difference between the Pt and TiN_{1-x} ORR current is greater when the substrate potential is more negative due to the difference in their ORR kinetics. For this reason, a substrate potential lower than -0.15 V normally will be applied in the following section to avoid very low ORR current efficiency.

3.4. The effect of tip–substrate separation on SECM images

The factor of tip–substrate separation should also be considered when studying oxygen reduction with the current modified TG–SC mode SECM. Theoretically in the current TG–SC mode, when the tip–substrate separation is less than two times the tip radius (here $12.5\ \mu\text{m}$), the tip-generated species (oxygen) predominately diffuses to the substrate surface, instead of escaping from the gap between the tip and the substrate [21]. At greater tip–substrate distance, more oxygen will diffuse into the bulk solution and cannot reach the substrate. As the result, the ORR current efficiency from the substrate is expected to decrease with increasing tip–substrate distance. At the same time, the SECM image resolution is higher when the tip–substrate distance is smaller. However, if the tip–substrate distance is too small, image distortion may occur, as described in Ref. [19], where feature elongation along the scan direction was observed when the separation distance was $5\ \mu\text{m}$. The feature distortion was attributed to the oxygen still remaining between the substrate and the glass sheath of the tip after the tip had already moved several micrometers away.

The effect of tip–substrate separation on the SECM image can be seen from Fig. 8, where SECM images at 15, 30, 50, 70, and $100\ \mu\text{m}$ tip–substrate distances are shown. It can be observed that SECM images with reasonable resolution can be obtained when the tip–substrate separation is in the range of 15 – $70\ \mu\text{m}$. This indicates that images obtained in TG–SC mode are not as sensitive to variations in the tip–substrate distance as in feedback mode SECM measurements, which is consistent with previous literature reports [19]. Careful examination of these SECM images allows for some additional observations. First, as shown in a plot of maximum net substrate current as a function of the tip–substrate separation in Fig. 9, the net substrate current

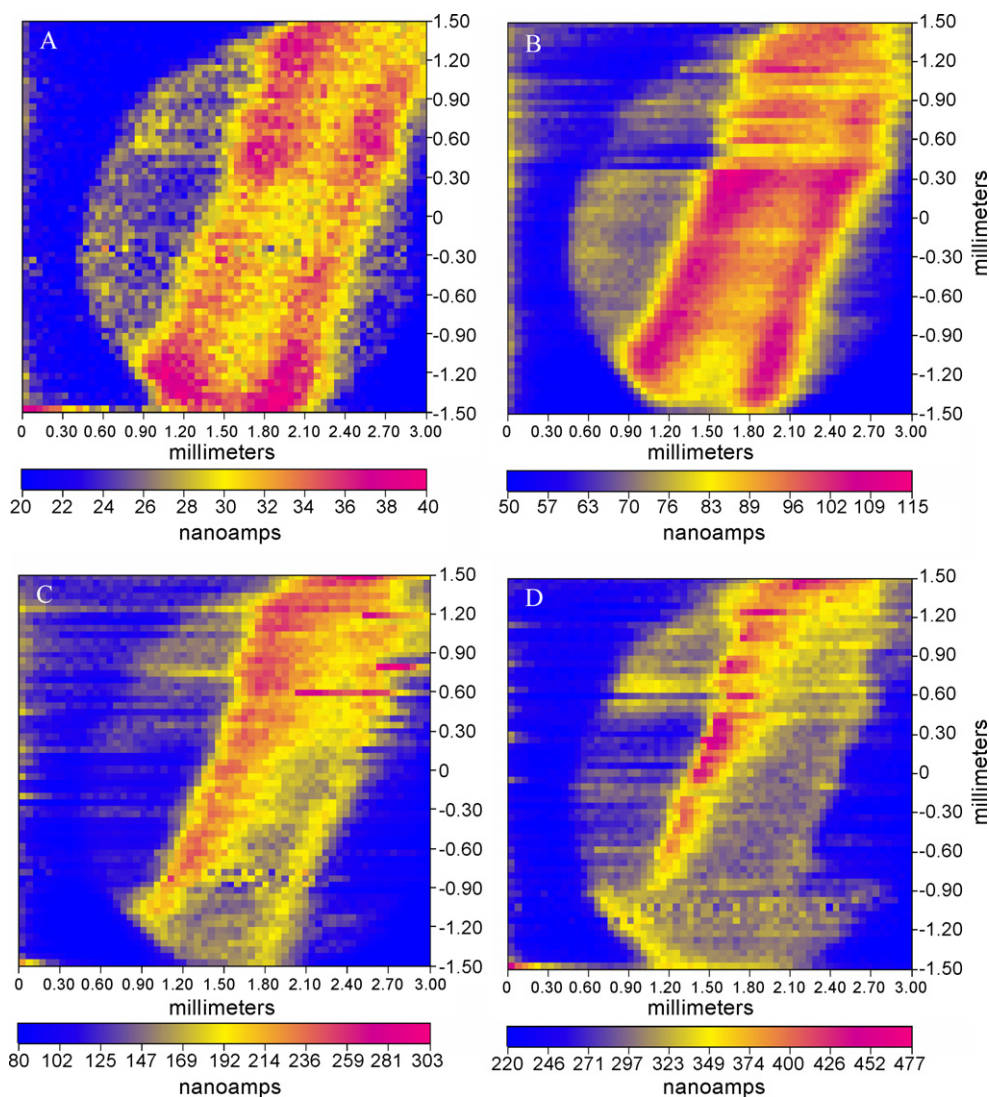


Fig. 6. Area scan ORR images obtained by TG–SC SECM of a Pt stripe in 0.5 M H_2SO_4 when the substrate potential is different. (A) $E_{\text{sub}} = 0.1 \text{ V}_{\text{SCE}}$, $I_{\text{tip}} = 179 \text{ nA}$; (B) $E_{\text{sub}} = 0 \text{ V}_{\text{SCE}}$, $I_{\text{tip}} = 178 \text{ nA}$; (C) $E_{\text{sub}} = -0.15 \text{ V}_{\text{SCE}}$, $I_{\text{tip}} = 177 \text{ nA}$; (D) $E_{\text{sub}} = -0.25 \text{ V}_{\text{SCE}}$, $I_{\text{tip}} = 178 \text{ nA}$. In all cases, the tip–substrate separation is $15 \mu\text{m}$.

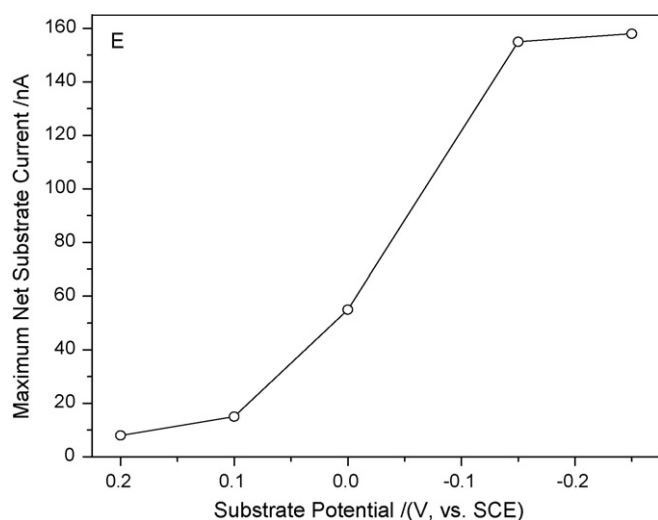


Fig. 7. Maximum net substrate ORR current as a function of substrate potential for line scan results obtained from Fig. 5 along the line of y coordinate of -0.6 mm .

decreases with increasing tip–substrate separation. This can be easily understood by considering that with longer tip–substrate separation, more oxygen will diffuse into the bulk solution before reaching the substrate surface. As a result, more oxygen will be accumulated in the solution, which also explains the larger background current noise and lower image quality at the later stages of tip scanning in the case of the $100 \mu\text{m}$ distance sample. Secondly, the SECM image contrast ratio is improved with increasing separation up to $70 \mu\text{m}$, despite the net substrate current decrease with increasing distance, which results in the gradual disappearance of the circular shape of the TiN layer.

Although TG–SC SECM imaging is not very sensitive to the tip–substrate separation, there is a concern about image distortion when the tip is brought very close to the substrate, as noted earlier. In the present study, the tip was brought to a $5 \mu\text{m}$ separation from the substrate and a SECM image was obtained with a substrate potential of 0 V , as shown in Fig. 10. As can be seen, the image resolution is relatively good and minimal image distortion is observed. The discrepancy with the reported results

is probably because the tip scanning rate of the current study ($50 \mu\text{m/s}$) is much slower than in the reported work ($300 \mu\text{m/s}$) [19].

Extensive investigation of continuous thin film composition spread combinatorial libraries of binary and ternary Pt-based alloy materials for the ORR and exploration of better and less-costly cathodic catalyst compositions for PEM fuel cells are being conducted and will be the subjects of further communications.

3.5. Further discussion and concluding remarks

As discussed above, the modified TG–SC mode SECM technique (with constant tip current from an outside source) can be used to rapidly and efficiently screen thin film materials for their electrocatalytic activity towards oxygen reduction in acidic media. Compared to feedback mode SECM, TG–SC mode has the following advantages.

Firstly, the main advantage is that it does not rely on a feedback process. This is convenient for investigating reactions that are not able to be studied by feedback mode SECM, like the ORR in acidic media in this work.

Secondly, there are no limitations on the concentration of the electrolytes used. In the feedback mode, the concentration of the bulk electrolyte has to be very dilute so that the tip reaction is under diffusion control and the concentration change of certain specie due to the diffusion from the substrate reaction, can be discerned. This is sometimes not acceptable since SECM data acquired in solutions with much smaller concentrations may not represent the real situation in a more concentrated solution if the kinetics of the reaction of interest are concentration dependent. Feedback mode is even less well suited if one has to consider the stability and corrosion resistance of alloy libraries, since there is a strong correlation between the corrosion resistance and the environmental media. In the case of hydrogen oxidation, the electrolyte used has to be $0.01 \text{ M H}_2\text{SO}_4$ to maintain a

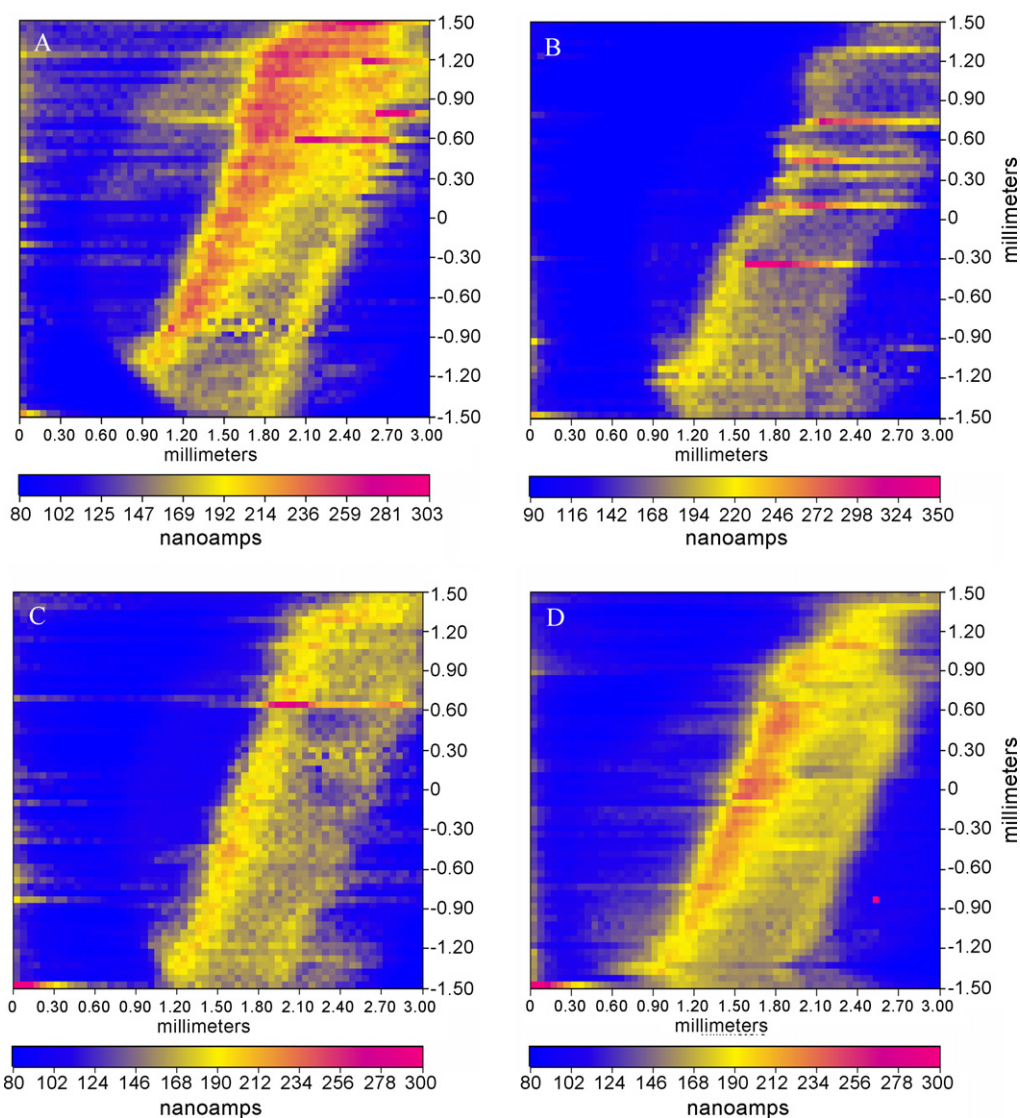


Fig. 8. Area scan ORR images obtained by TG–SC SECM of a Pt stripe in $0.5 \text{ M H}_2\text{SO}_4$ when the tip–substrate separation is different. (A) $d = 15 \mu\text{m}$, $I_{\text{tip}} = 177 \text{ nA}$; (B) $d = 30 \mu\text{m}$, $I_{\text{tip}} = 176 \text{ nA}$; (C) $d = 50 \mu\text{m}$, $I_{\text{tip}} = 175 \text{ nA}$; (D) $d = 70 \mu\text{m}$, $I_{\text{tip}} = 181 \text{ nA}$; (E) $d = 100 \mu\text{m}$, $I_{\text{tip}} = 179 \text{ nA}$. In all cases, the substrate potential is kept at -0.15 V .

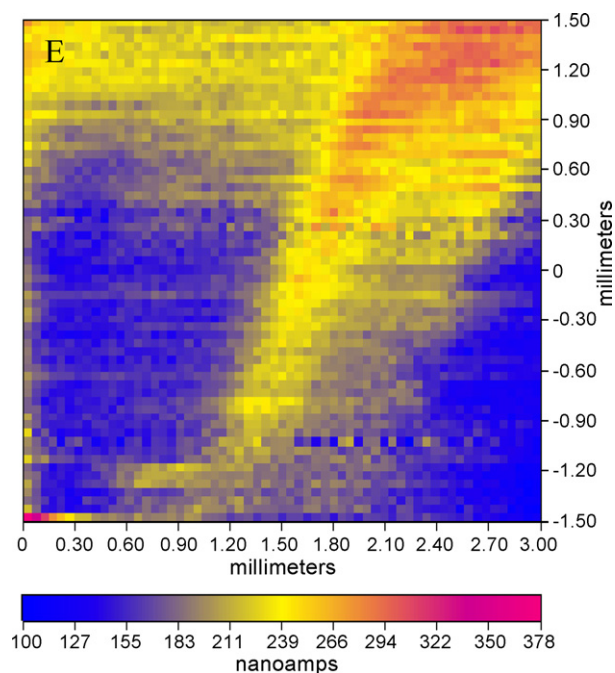


Fig. 8. (Continued)

diffusion-limited condition and avoid hydrogen bubble formation, instead of 0.5 M H_2SO_4 , a solution widely used to mimic the acidic environment in a PEM fuel cell system. To increase the ionic conductivity of the solution, 0.1 M NaSO_4 is added. In the TG–SC mode explored here, solutions with high concentration are acceptable. In the case of ORR, 0.5 M H_2SO_4 can be used.

Thirdly, in TG–SC mode, the tip–substrate separation is not necessarily as close as in the case of SECM feedback mode study on HOR. As discussed above, the TG–SC mode is less sensitive to variations of tip–substrate separation than the feedback mode, in which the sample leveling is very critical to avoid image fading due to troublesome substrate topography effects and possible changes in tip–substrate separation during SECM characterization. The highly nonlinear tip current response to

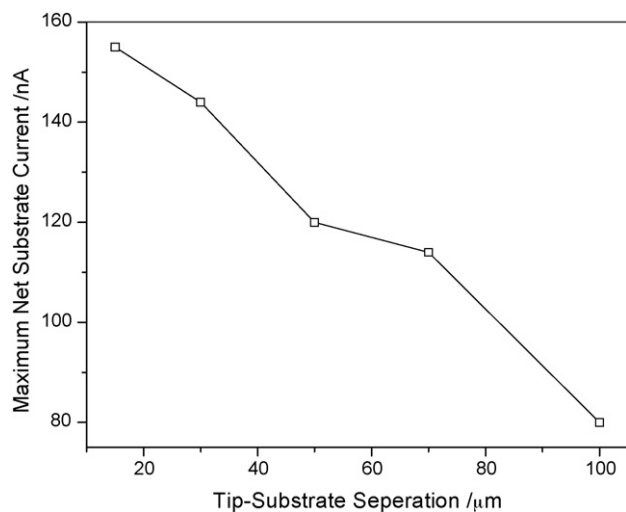


Fig. 9. Maximum net substrate ORR current as a function of tip–substrate separation for line scan results obtained from Fig. 7 along the line of y coordinate of -0.6 mm .

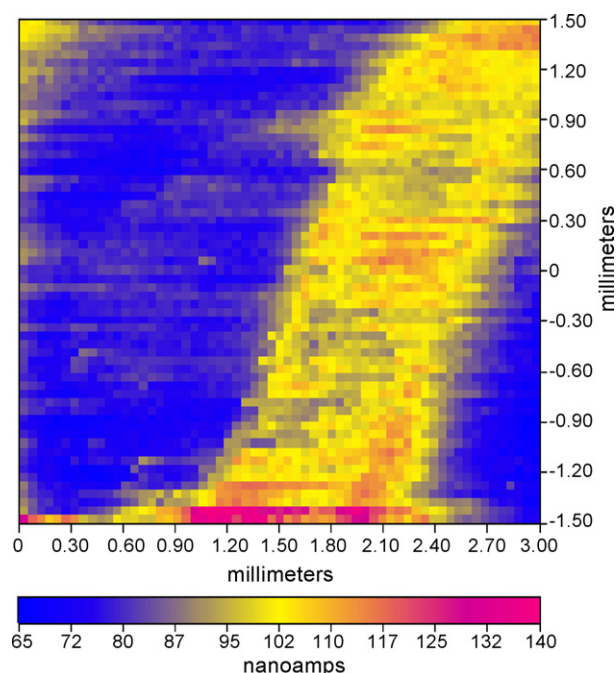


Fig. 10. Area scan ORR images obtained by TG–SC SECM of a Pt stripe in 0.5 M H_2SO_4 with the tip–substrate separation as $5\text{ }\mu\text{m}$, $I_{\text{tip}} = 175\text{ nA}$, $E_{\text{sub}} = 0\text{ V}_{\text{SCE}}$.

tip–substrate separation in both positive and negative feedback presents some difficulties interpreting the SECM images with respect to reaction rate. Because of that, in feedback mode SECM, a very time-consuming and tedious physical leveling of the substrate relative to the plane of tip travel is critically necessary. This limits the ability to accurately and quickly evaluate composition libraries unless a control unit, such as a tip height sensor, is installed to give constant tip–substrate distance and overcome this limitation. In TG–SC mode SECM, rough sample leveling of the substrate is sufficient before the characterization. More importantly, this feature of TG–SC mode makes it possible to use TG–SC mode SECM to characterize surfaces that are not as flat as Si wafers. This method can be extended to porous systems, as long as the conductive area is controlled to be small to avoid high background current.

Finally, the TG–SC mode described here is more tolerant of contamination of the tip surface than the traditional feedback mode, since the function of the tip here is just to pass current and generate oxygen. The potential of the tip is not controlled and the kinetics of the reaction that occurs on the tip is not the one of interest. It is the substrate surface that plays a critical role in studying oxygen reduction. The surface has to be cleaned by CV before every experiment to maintain the same surface status. In feedback mode SECM, tip fouling due to tip contamination from impurities in the electrolyte is a notorious problem and causes time-dependent effects in SECM images, which is not desirable, especially when the characterization takes long time [11,23].

Acknowledgements

This work described herein was financially supported by the U.S. Army CECOM RDEC through Agreement No. DAAB07-

03-3-K414. Such support does not constitute endorsement by the U.S. Army of the views expressed in this publication. It was also partially supported through funding from the Indiana 21st Century Technology and Research Fund.

The authors are grateful to Dr. Allen J. Bard of University of Texas at Austin and two of his coworkers Jose L. Fernandez and Mario A. Alpuche for kind suggestions and insightful discussion. Yu Cao and Kai Sun of EE Dept. of University of Notre Dame are also greatly appreciated for helping the AFM measurements.

References

- [1] T. Toda, H. Igarashi, H. Uchida, M. Watanabe, *J. Electrochem. Soc.* 146 (1999) 3750.
- [2] U. Paulus, A. Wokaun, G.G. Scherer, T.J. Schmidt, V. Stamenkovic, V. Radmilovic, N.M. Markovic, P.N. Ross, *J. Phys. Chem. B* 106 (2002) 4181.
- [3] E. Reddington, A. Sapienza, B. Gurau, R. Viswanathan, S. Sarangapani, E.S. Smotkin, T.E. Mallouk, *Science* 280 (1998) 1735.
- [4] R. Jiang, D. Chu, *J. Electroanal. Chem.* 527 (2002) 137.
- [5] J. Zhou, Y. Zu, A.J. Bard, *J. Electroanal. Chem.* 491 (2000) 22.
- [6] S. Jayaraman, A.C. Hillier, *J. Comb. Chem.* 6 (2004) 27.
- [7] B.C. Shah, A.C. Hillier, *J. Electrochem. Soc.* 147 (2000) 3043.
- [8] C.G. Zoski, *J. Phys. Chem.* 107 (2003) 6401.
- [9] S. Jayaraman, A.C. Hillier, *J. Phys. Chem.* 107 (2003) 5221.
- [10] M. Prochaska, J. Jin, D. Rochefort, L. Zhuang, F.J. Disalvo, H.D. Abruna, R.B. Van Dover, *Rev. Sci. Instrum.* 77 (2006) 054104.
- [11] M. Black, J. Cooper, P. McGinn, *Chem. Eng. Sci.* 59 (2004) 4839.
- [12] M. Black, J. Cooper, P. McGinn, *Meas. Sci. Technol.* 16 (2005) 174.
- [13] J.S. Cooper, G. Zhang, P.J. McGinn, *Rev. Sci. Instrum.* 76 (2005) 062221.
- [14] G. Lu, J.S. Cooper, P.J. McGinn, *J. Power Sources* 161 (2006) 106.
- [15] J.L. Fernandez, D.A. Walsh, A.J. Bard, *J. Am. Chem. Soc.* 127 (2005) 357.
- [16] Y.X. Wang, P.B. Balbuena, *J. Phys. Chem. B* 109 (2005) 18902.
- [17] G. Chen, D.A. Delafuente, S. Sarangapani, T.E. Mallouk, *Catal. Today* 67 (2001) 341.
- [18] B. Liu, A.J. Bard, *J. Phys. Chem. B* 106 (2002) 12801.
- [19] J.L. Fernandez, A.J. Bard, *Anal. Chem.* 75 (2003) 2967.
- [20] D.A. Walsh, J.L. Fernandez, A.J. Bard, *J. Electrochem. Soc.* 153 (2006) E99.
- [21] A.J. Bard, M.V. Mirkin, *Scanning Electrochemical Microscopy*, Marcel Dekker, New York, 2001.
- [22] J.S. Cooper, P.J. McGinn, Unpublished multichannel microelectrode data regarding oxygen reduction.
- [23] C.G. Zoski, *Anal. Chem.* 76 (2004) 62.